Annex no 4 (English version)

Summary of research achievements

Sławomir Kubacki, PhD

1. Name and Surname

Sławomir Kubacki

2. Diplomas and scientific degrees - including name, place and year of obtaining the degree, title of PhD thesis. Provide the thesis supervisor and referees.

PhD in Mechanics,
Częstochowa University of Technology,
Institute of Thermal Machinery, Faculty of Mechanical Engineering and Computer Science, 2005

Title of PhD thesis: *Parallel computing in analysis of the Navier-Stokes equations using spectral methods*

supervisor – prof. Andrzej Bogusławski
referee – prof. Jacek Rokicki
referee – prof. Norbert Sczygiol

MSc in Mechanics, major Energy Engineering
Częstochowa University of Technology,
Institute of Thermal Machinery, Faculty of Mechanical Engineering and Computer Science, 2000

3. Work in academic institutions

X.2009–obecnie	Warsaw University of Technology, Institute of Aeronautics and Applied Mechanics, *assistant professor (adjunct)*
X.2006–IX.2009	Universiteit Gent (Ghent University), Vakgroep Mechanica van Stroming, Warmte en Verbranding, (Department of Flow, Heat and Combustion Mechanics), Ghent, Belgium *post-doc*
IV.2001–III.2006	Częstochowa University of Technology, Institute of Thermal Machinery, *PhD student*

4. Achievements in the discipline *Mechanics* as provided for in Article 16 (2) of the Act of March 14, 2003 on Academic Degrees and Academic Title and Degrees

Title of research achievement:

Hybrid RANS/LES method and laminar to turbulent transition model in simulation of steady and unsteady internal flows

List of publications consists of research achievement:

H1: Kubacki S., Dick E., 2016, An algebraic model for bypass transition in turbomachinery boundary layer flows, *International Journal of Heat and Fluid Flow*, 58, 68–83.
[**IF_{2015}:1.737**, contribution 70%, elaboration of the model for prediction of laminar-turbulent transition, carry out the simulations, analysis of results]

H2: Kubacki S., Dick E., 2010, Simulation of plane impinging jets with $k-\omega$ based hybrid RANS/LES models, *International Journal of Heat and Fluid Flow*, 31, 862-878.
[**IF_{2010}:1.802**, contribution 70%, development of the hybrid RANS/LES techniques based on the RANS k-ω model, carry out the simulations, analysis of results]

H3: Kubacki S., Rokicki J., Dick E., 2011, Hybrid RANS/LES computation of plane impinging jet flow, *Archives of Mechanics*, 63 (2) 117-136.
[**IF_{2011}:0.396**, contribution 65%, development of the hybrid RANS/LES techniques based on the RANS k-ω model, carry out the simulations, analysis of results]

H4: Kubacki S., Dick E., 2011, Hybrid RANS/LES of flow and heat transfer in round impinging jets, *International Journal of Heat and Fluid Flow*, 32, 631-651.
[**IF_{2011}:1.927**, contribution 70%, development of the hybrid RANS/LES techniques based on the RANS k-ω model, carry out the simulations, analysis of results]

H5: Kubacki S., Rokicki J., Dick E., 2013, Predictions of round impinging jet heat transfer with two k-ω hybrid RANS/LES models, 2013, *International Journal of Numerical Methods for Heat and Fluid Flow,* 23 (6), 1023-1048.
[**IF_{2013}:0.919**, contribution 65%, development of the hybrid RANS/LES techniques based on the RANS k-ω model, carry out the simulations, analysis of results]

H6: Kubacki S., Rokicki J., Dick E., 2013, Hybrid RANS/LES computations of plane impinging jets with DES and PANS models, *International Journal of Heat and Fluid Flow*, 44, 596 - 609.
[**IF_{2013}:1.777**, contribution 65%, development of the hybrid RANS/LES techniques based on the RANS k-ω model, carry out the simulations, analysis of results]

H7: Kubacki S., Rokicki J., Dick E., 2016, Simulation of the flow in a ribbed rotating duct with a hybrid k-ω RANS/LES model, *Flow Turbulence and Combustion*, 97, 45–78.
[**IF_{2015}:1.863**, contribution 65%, development of the DES technique based on the RANS k-ω model, carry out the simulations, analysis of results]

H8: Kubacki S., Dick E., 2009, Convective heat transfer prediction for an axisymmetric jet impinging onto a flat plate with an improved k-ω model, *International Journal of Numerical Methods for Heat and Fluid Flow*, 19 (8) 960-981.
[**IF_{2009}:0.790**, contribution 70%, elaboration of correction terms for improvement of the k-ω model in stagnation flow region, analysis of results]

H9: Kubacki S., Dick E., 2010, Convective heat transfer predictions in an axisymmetric jet impinging onto a flat plate using an improved k-ω model, *Journal of Computational and Applied Mathematics*, 234 (7) 2327-2335.
[**IF_{2010}:1.030**, contribution 70%, elaboration of correction terms for improvement of the k-ω model in stagnation flow region, analysis of results]

H10: Kubacki S., Dick E., 2011, Simulation of impinging jet mass transfer at high Schmidt number with algebraic models, *Progress in Computational Fluid Dynamics*, 11 (1) 30-41.
[**IF_{2011}:0.298**, contribution 70%, elaboration of correction terms for improvement of the mass transfer prediction using the k-ω model, analysis of results]

Goal of the research activities, obtained results and their possible use

Summary

Research activities focused on development of a new, algebraic, laminar-turbulent transition model and its incorporation into a newest version of RANS (Reynolds-averaged Navier-Stokes) k-ω model by Wilcox (2008), improvement of convective heat and mass transfer characteristics using the k-ω model, and analysis of various k-ω based hybrid RANS/LES models (Large Eddy Simulation) for simulation of benchmark flows, [**H1**-**H10**].

Modeling of laminar to turbulent (L-T) transition in boundary layer flows is relevant in many academic and engineering applications in which an accurate estimation of losses associated with development of the boundary layers is required. Examples are flows over blades of low pressure turbines and compressors or flows over wings of aircrafts at $Re=5\cdot10^4$-10^6 (Reynolds number based on chord length). Turbomachinery flows are commonly modeled using the RANS models (k-ε, k-ω, SST), which treat the whole flow field as fully turbulent. In some cases, an assumption of fully turbulent flow may lead to differences between predicted and measured boundary layer losses, as significant parts of developing boundary layers stay laminar (laminar flow may occur for 30-90% of the blade surface length). A reduction of the number of blades in rows of turbines and compressors necessities an application of highly loaded blades. This increases a risk of laminar boundary layer separation. Such phenomenon cannot be fully captured with the classical fully turbulent models, which suppress the flow instabilities in separated laminar boundary layers. As result, the associated pressure losses might be underestimated using the fully turbulent RANS models. The development of accurate RANS models, able to take into account the laminar portions of the boundary layers is, therefore, important in design process of turbomachines. In [**H1**] a development of new, simple, algebraic model for prediction of bypass transition mechanism in attached boundary layer flow was considered. The bypass transition occurs in boundary layer flows subjected to high freestream turbulence level, Tu > 1% ($Tu=u'/U_\infty$, u' - rms of fluctuating velocity component at edge of the boundary layer, U_∞ - mean velocity at edge of the boundary layer), which is typical for turbomachinery flows. So the bypass transition, and the separation-induced transition, are typical transitions mechanisms which take place in turbomachinery applications. It is, therefore, important to develop a robust and accurate model for bypass transition prediction.

Development of the hybrid RANS/LES models is relevant in simulation of high Reynolds number flows characterized by complex flow dynamics away from walls. Examples are simulation of stalled airfoil or flow inside the combustion chamber of aircraft engine. Again, an application of classical RANS models for simulation of such complex flows and related processes is questionable and may lead to differences with

respect to experiment, both in estimation of overall pressure losses or predicted heat transfer characteristics. In contrast, the hybrid RANS/LES models allow for accurate resolution of the flow physics in the flow regions which are far from equilibrium. This necessitates an application of sufficiently fine meshes in order to properly activate the LES mode of the hybrid model in critical flow regions. The role of the underlying subgrid model is, therefore, limited in the critical flow regions, as most of the turbulence is resolved there. Near to walls the hybrid RANS/LES model switches into the RANS mode and the small-scale turbulent motion is fully modelled there. The computational costs associated with an application of the hybrid RANS/LES models are much less than using the wall-resolved LES. This is due to possibility to use much coarser meshes in the near wall region with the hybrid model than with LES. The grid densities which have been employed for simulations of turbulent flows in [**H2-H7**] using the hybrid RANS/LES models consisted from few up to dozen million of cells. An application of LES/DNS methods for simulation of above flows will require much denser grids with tens or hundreds million of cells (Hadziabdic i Hanjalic, 2008, Sandberg i in., 2015). The reduction of the number of degrees of freedom with application of the hybrid models is, therefore, significant.

In [**H1**] the new algebraic model has been proposed for prediction of bypass transition in boundary layer flows. The model has been developed based on the concept of secondary instability of Klebanoff modes. The model uses only local variables, available in each cell of computational domain, and is well suited for implementation on parallel computers. It was demonstrated that filtering of high-frequency disturbances by the boundary layer shear can be modeled using a simple criteria based on comparison of two time scales: time scale of wall normal diffusion and the time scale characterizing the mean flow. Both time scales have a physical interpretation which is determined from DNS of bypass transition. The turbulence breakdown process is modeled using a simple criteria based on comparison of two velocity scales: velocity scale of turbulent disturbances and the velocity scale of wall-normal diffusion process. Good agreement has been obtained between measurements and simulation using 2D RANS and 3D URANS techniques in analysis of benchmark flat plate flows as well as in simulation of flow through turbine and compressor cascades. The developed algebraic model [**H1**] is characterized by much less complexity than the one- or two-equation laminar to turbulent transition models which are currently available in commercial packages (ANSYS Fluent, ANSYS CFX).

Different hybrid RANS/LES techniques were studied in [**H2**-**H7**] for simulation of plane and round impinging jet flows and convective heat transfer and the flow inside the rotating ribbed channel. The study of above problems is relevant in many turbomachinery applications (flow in blade passages of radial compressors and in internal cooling channels of rotating blades in axial turbine stages of gas turbine engines). An improvement to the hybrid RANS/LES model by Kok et al. (2004) has been proposed for flow simulation on anisotropic grids employing the two different measures of the local grid size: one in destruction term of k-equation and one in the eddy viscosity formula. It was shown that an adequate subgrid viscosity level is obtained with the hybrid RANS/LES models which allow to impose in a direct way the small-scale Smagorinsky limit on fine enough grids by equating production and dissipation in the k-equation or both in k- and ω-equations. The boundary conditions have been derived for modeled scalars at inlet to the computational domain. Insight into the flow physics was gained in stagnation flow region for simulation of round impinging jet flow and

convective heat transfer at small distance between the nozzle exit and plate (H/D=2, D - nozzle diameter). It was demonstrated, that a generation of secondary vortices in the impingement flow region is initiated by primarily vortices coming from the shear layer of the jet. The development and breakdown of secondary vortices near to the wall has a significant role in enhancement of the heat transfer characteristics along plate and is responsible for appearance of secondary peak on the Nusselt number profile at radial distance r/D=2 (the first peak is visible at the jet axis). It was demonstrated that the hybrid RANS/LES models are able to overcome the deficiencies of the RANS techniques both for simulation of free shear flows and for simulation of flow in the stagnation flow regions.

In [**H8**] and [**H9**] the improvements have been introduced into the k-ω model (Wilcox, 2008) in order to correct the heat transfer characteristics in the stagnation flow region for simulation of the round impinging jet flows. The corrections allowed to obtain a more accurate results at low nozzle-plate distance (H/D=2). It was possible to reproduce the two peaks, one at r/D=0 and the second at r/D=2, on the Nusselt number profile along the plate using the modified k-ω model. A simple algebraic model was proposed in [**H10**] for prediction of impinging jet mass transfer at high Schmidt number. The improvement was based on modification of the diffusion coefficient in the transported scalar equation. The obtained results [**H8-H10**] were in good agreement with experimental data. Detailed description of achieved results is presented below.

Model for prediction of laminar to turbulent boundary layer transition

In last two decades a significant progress has been made in development of the laminar to turbulent transition models for prediction of the boundary layer flows using the RANS techniques. In transition modeling it is important to capture both the transition onset and the growth rate of fluctuations in a pseudolaminar boundary layer. The first transition models were based on modification of the eddy-viscosity based RANS models in order to properly reproduce the growth rate of turbulent shear stress in transition zone. This allowed for modeling of the length of transition zone. The transition onset itself was frequently determined using the Abu-Ghannam and Shaw (1980) and Mayle (1991) correlations or using the experimental data. Examples are models by Schmidt and Patankar (1991) and Wilcox (1992). Schmidt and Patankar (1991) proposed a modification to the production term in the k-equation using the experimental correlations for growth rate of disturbances in pseudolaminar boundary layer. Wilcox (1992) developed the so called transitional version of the k-ω model for prediction of natural transition mechanism. The natural transition is initiated in attached boundary layer by 2D viscosity dependent Tollmien-Schlichting instability waves, leading to the formation of 3D spanwise periodic Λ-vortices, which further downstream break down into turbulent spots. In the Wilcox model this process was taken into account in simplified manner by adjusting the model constants.

In last decade a number of intermittency based models have been proposed. The intermittency function γ equals zero in laminar flow and unity in the fully turbulent flow. An application of the intermittency function was suggested by Steelant and Dick (1996), as alternative to the approach based on conditionally-averaged Navier-Stokes equations. In Steelant and Dick (1996) the transition onset was determined using correlations, but

evolution of turbulent fluctuations in transitional flow region was governed by solution of separate convection-diffusion-source equation for the intermittency function. Later, this technique was adopted by Menter et al. (2002), Langtry and Menter (2006), Lodefier et al. (2006) and Durbin (2012) for construction of their own intermittency models based on local variables. Langtry and Menter (2006) in addition to the intermittency transport equation solved also the second equation for evolution of the momentum thickness Reynolds number, Re_θ. The model was named the γ-Re_θ model. The development of modeling approaches based on the γ-Re_θ model by Langtry i Mentera (2006) was continued by others (Suluksna et al., 2009, Piotrowski et al., 2010). As said, the Langtry and Menter (2006), Lodefier et al. (2006), Durbin (2012) and Menter et al. (2015) models are based on local variables (they employ variables which are available in each cell of computational domain), so they are well suited for simulation of transitional flows on parallel computers (domain decomposition). The models by Langtry and Menter (2006), Lodefier et al. (2006), Durbin (2012) and Menter et al. (2015) are meant for prediction of both natural and bypass transition. Bypass transition occurs in flows with high freestream turbulence level (Tu > 1%). Under the influence of free stream turbulence, streamwise elongated disturbances are induced in the near wall zone of a laminar boundary layer. Zones of forward and backward jet-like perturbations alternate in spanwise direction, with almost perfect periodicity, termed streaks or Klebanoff modes. The Klebanoff distortions grow downstream both in length and amplitude and finally break down with formation of turbulent spots. The transition is then called of bypass type, which means that the instability mechanism of the Tollmien-Schlichting waves is bypassed. Modeling of bypass transition is relevant in turbomachinery flows at Reynolds number (based on chord length and inlet velocity) varying from $5 \cdot 10^4$ to 10^6, and a development of algebraic model for bypass transition prediction was a subject of present work [**H1**].

The models by Langtry and Menter (2006, 2009) and Menter et al. (2015) employ in an indirect way the experimental correlations for transition onset prediction. Different technique was proposed by Walters and Laylek (2004), using a concept by Mayle and Schultz (1997). Mayle and Schultz (1997) suggested a modeling of the laminar fluctuations in pretransitional boundary layer by solution of transport equation. Walters and Laylek (2004) constructed a reliable model for production and development of fluctuations in laminar boundary layer based on the k-ε model. The equation for development of fluctuating velocity component can be derived from equation for wall-parallel Reynolds stress component. In Walters and Laylek (2004) the transition onset was modelled by transfer of energy from laminar to turbulent fluctuations. Later, Walters and Cokljat (2008) transformed the laminar kinetic energy model by Walters and Laylek (2004) to the k-ω framework. Simpler version of the laminar kinetic energy model has been derived by Pacciani et al. (2011). The models by Walters and Cokljat (2008), similar to the model by Langtry and Menter (2006), give reliable results for simulation of aerodynamic and turbomachinery flows, but they are very complex. For instance, the model by Walters and Cokljat (2008) uses more than twenty functions and more than dozen of constants for modelling of the bypass transition. The models by Walters and Cokljat (2008) and Langtry and Menter (2006) are, therefore, difficult to implement in CFD codes owing to complexity of their formulation. So in [**H1**] efforts were made to derive much simpler technique for prediction of bypass transition.

In [**H1**] a new algebraic transition model has been proposed for modeling of the bypass transition. The model is based on modification of the production terms in the k-ω

model. The model ingredients have been obtained based on DNS data and results of linear stability analysis employed in the flow region before transition onset (Jacobs and Durbin, 1998, 2001, Brandt et al. 2004, Zaki and Durbin, 2005, 2006, Zaki, 2013). The transport equations for the turbulent kinetic energy and specific dissipation rate are

$$\frac{Dk}{Dt} = \gamma \nu_s S^2 - \beta^* k\omega + \frac{\partial}{\partial x_j}\left[\left(\nu + \sigma^* \frac{k}{\omega}\right)\frac{\partial k}{\partial x_j}\right], \tag{1}$$

$$\frac{D\omega}{Dt} = \alpha \frac{\omega}{k}\nu_s S^2 - \beta\omega^2 + \frac{\partial}{\partial x_j}\left[\left(\nu + \sigma \frac{k}{\omega}\right)\frac{\partial \omega}{\partial x_j}\right] + \frac{\sigma_d}{\omega}\frac{\partial k}{\partial x_j}\frac{\partial \omega}{\partial x_j}. \tag{2}$$

The factor γ is a multiplier of the production term in the k-equation. We call it the intermittency factor, in analogy with the factor used in typical intermittency transition models. However, technically, it is solely a starting function for the turbulence. The production term itself is $\nu_s S^2$, where ν_s is the small-scale eddy viscosity, which is part of the full eddy viscosity ν_T. The introduction of γ and ν_s are the only fundamental changes to the k-ω model. In the laminar part of a boundary layer, γ is set to zero. There is then no production of k, but turbulent kinetic energy enters by diffusion out of the free-stream flow. In the laminar part of a boundary layer, the ω-equation stays active. This is allowed since, as proven by Wilcox, the ω-equation has a non-zero laminar-flow solution for vanishing k and eddy-viscosity.

The algebraic model takes into account two effects: filtering of high-frequency free-stream disturbances by shear and breakdown of near-wall disturbances known as Klebanoff modes (Klebanoff, 1971) into fine-scale turbulence. The filtering process of high-frequency disturbances is known as the shear-sheltering effect (Jacobs i Durbin, 1998). It was demonstrated that this process can be modelled using a simple criteria based on comparison of two time scales: time scale of wall-normal diffusion and the time scale characterizing the mean flow (convective time scale).

Walters and Cokljat (2008) assume that the convective time scale is the time scale of the strain, $\tau_c = 1/\Omega$, where Ω is the invariant of the vorticity tensor, i.e. $\Omega = (2\Omega_{ij}\Omega_{ij})^{1/2}$, with $\Omega_{ij} = 1/2(\partial U_i/\partial x_j - \partial U_j/\partial x_i)$. The diffusive time scale is fundamentally ℓ_d^2/ν, with ℓ_d the diffusive length scale and ν the kinematic fluid viscosity. For fluctuations in the outer part of a laminar boundary layer, this length scale was estimated by Walters (2009), assuming proportionality between $\sqrt{k}/\ell_d$, where $\sqrt{k}$ is the velocity scale of the fluctuations, and the mean velocity gradient, which is Ω. The results is $\ell_d \sim \sqrt{k}/\Omega$ and $\tau_d \sim k/\nu\Omega^2$. The ratio of the diffusive ($\tau_d \sim k/\nu\Omega^2$) and convective ($\tau_c = 1/\Omega$) time scales forms the Reynolds number $\mathrm{Re}_\Omega = k/(\nu\Omega)$. With this Reynolds number, Walters and Cokljat (2008) define a shear-sheltering factor as

$$f_{SS} = \exp[-(C_{SS}\,\nu\Omega/k)^2]. \tag{3}$$

where C_{SS} is a constant.

DNS results show that generation of Klebanoff modes (low speed streaks) is the result of penetration of low-frequency disturbances towards the inner part of boundary layer. The low-speed streaks lift away from the wall, causing local inflection of the streamwise velocity, both in wall-normal and spanwise directions. Consequently, low-

speed streaks are intrinsically unstable by inviscid Kelvin-Helmholtz-like instability. The breakdown of the low-speed streaks into small-scale structures leading to wall turbulence is initiated by the free-stream turbulence. This is called the secondary instability mechanism in contrast to the primarily instability mechanism associated with formation of streaks. Due to the inherent instability of the streaks, the breakdown into turbulence is much faster than with natural transition. In [**H1**] the secondary instability mechanism is modelled in simplified manner by comparison of two velocity scales: velocity scale of the turbulence $\sqrt{k}$ and the velocity scale of molecular diffusion for a diffusion length equal to the distance to the wall, thus ν / y:

$$\gamma = \min\left(\varsigma_T / A_T, 1\right), \qquad \varsigma_T = \max\left(\frac{\sqrt{k}\, y}{\nu} - C_T, 0\right), \tag{4}$$

where C_T i A_T are constants. The estimation of velocity scale for wall-normal diffusion has been considered following Zaki (2013). Summing up, the shear sheltering term (3) damps the high-frequency oscillations coming from the outer parts of the boundary layer while the function (4) models the turbulence breakdown. Results show that taking into account the above processes is sufficient for capturing the bypass transition process.

The model has been tuned for the flat plate T3C cases of ERCOFTAC, relevant for bypass transition and tested for flow through cascades of N3-60 ($\mathrm{Re}=6\times10^5$) steam turbine stator vanes, V103 ($\mathrm{Re}=1.385\times10^5$) compressor blades and T106A ($\mathrm{Re}=1.6\times10^5$) gas turbine rotor blades. The transition model produced good results for bypass transition in attached boundary layer state and in separated boundary layer state for flows of elevated free-stream turbulence, both for 2D steady RANS and 3D time-accurate RANS simulations. Good results were also obtained for transition in separated laminar boundary layers at low free-stream turbulence by 3D time-accurate RANS simulations, thanks to resolution of the boundary layer instability and the beginning of the breakdown of the generated spanwise vortices. The model showed a good sensitivity to change of the turbulent length at the inlet to the computational domain and the obtained results were in good agreement with correlations by Mayle (1991) and Langtry i Menter (2009).

Fig. 1 shows the shape factor profile obtained for simulation of flow over N3-60 blade at two turbulence levels [**H1**]. Fig. 1 (a) shows that a good correspondence has been obtained between measurement and prediction for simulation of bypass transition ($S/S_0=0.75$) at high turbulence level, Tu=3%. Fig. 1 (b) shows also a good agreement between measurement and simulation obtained with the 3D URANS technique at a low freestream turbulence level, Tu=0.4%. In this case the transition is not modeled but is resolved (similar to LES).

The developed model can be, therefore, employed for prediction of bypass transition mechanism in turbomachinery flows using 2D RANS/3D RANS. For cases with laminar boundary layer separation one has to employ the 3D URANS technique in order to resolve the transition mechanism in separated boundary layer. The proposed model is much less complex than the transition models which are currently available in commercial packages (ANSYS Fluent, ANSYS CFX), so it can be considered as alternative to the models based on transport equations.

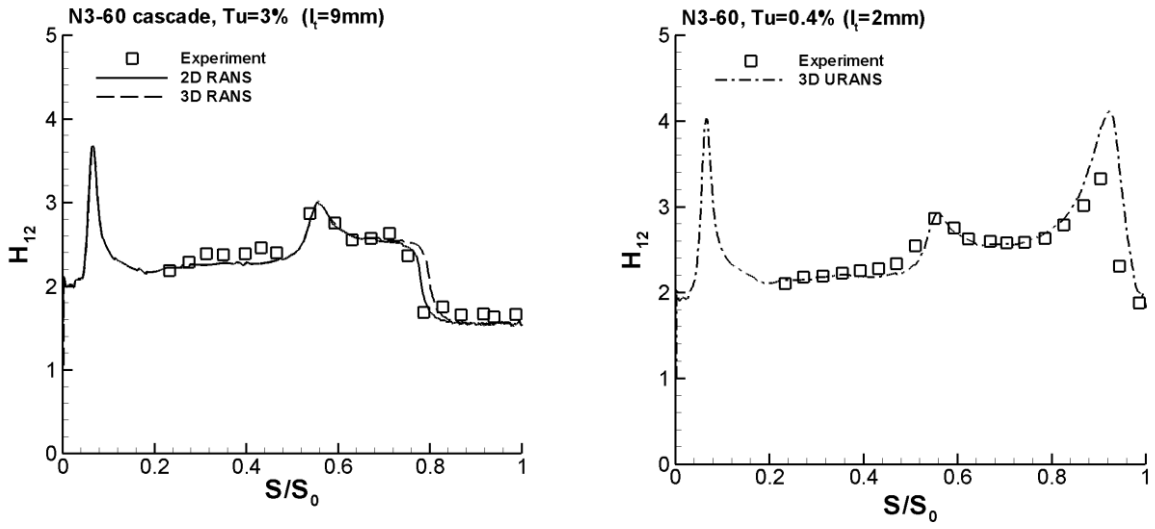

Fig. 1. Shape factor on suction side of N3-60 blade for different freestream turbulence levels. Left: Tu=3%, right: 0.4%. Results were obtained using the algebraic intermittency model [**H1**].

Hybrid RANS/LES techniques based on the k-ω model

Hybrid RANS/LES models are being more frequently applied for simulation of turbulent flows and prediction of convective heat transfer both in academic and industrial use. The hybrid models allow for resolution of the energy-bearing eddies away from walls and modelling of the small-scale structures in thin shear layers and close to walls using the RANS models. The numerical cost associated with application of the hybrid models is, therefore, much less than the cost associated with application of LES models thanks to modeling of the near-wall turbulent flow dynamics with the conventional RANS models. The reduced cost with the hybrid model is due to application of anisotropic grids near to walls (enlarged size of the near wall cells in the flow direction). The hybrid RANS/LES models analyzed in present work [**H2-H7**] belong to the class of continuous hybrid models. In continuous hybrid models it is not necessary to define, in an explicit way, the interfaces between RANS (unsteady RANS) and LES zones. It means a definition of coupling conditions at interfaces between RANS and LES zones is not required. Hereafter the name hybrid RANS/LES will be restricted to continuous hybrid RANS/LES model.

The first hybrid RANS/LES techniques have been proposed in late nineties by Speziale (1996) and Spalart et al. (1997). A significant contribution to development of hybrid models was done by Strelets (2001), Schiestel and Dejoan (2005), Chaouat and Schiestel (2005), Girimaji, (2006), Fadai-Ghotbi et al. (2010). So recently the hybrid RANS/LES models are considered as well-defined methods for prediction of turbulent flows (Fadai-Ghotbi et al., 2010). In present work [**H2-H7**], attempts were made to analyze and improve some characteristics of the various k-ω based hybrid RANS/LES models. In all the hybrid RANS/LES models the newest version of the k-ω model by Wilcox (2008) was used in the RANS mode. The model feasibility was demonstrated for

simulation of plane and round impinging jets. The study of convective heat transfer process near to impingement plate was also considered. Later, one of the studied hybrid models was employed for analysis of rib-roughened rotating channel flow.

Germano (1992) showed the averaging invariance of the Navier-Stokes equations based on application of the generalized central moments (eq. 5). He derived also the transport equations for the generalized central moments τ using the following relations (Moin i Yaglom, 1971):

$$\tau(u_i,u_j) = \langle u_i u_j \rangle - \langle u_i \rangle \langle u_j \rangle$$

$$\tau(u_i,u_j,u_k) = \langle u_i u_j u_k \rangle - \langle u_i \rangle \tau(u_j,u_k) - \langle u_j \rangle \tau(u_k,u_i) - \langle u_k \rangle \tau(u_i,u_j) - \langle u_i \rangle \langle u_j \rangle \langle u_k \rangle \quad (5)$$

where symbol < > denotes the averaging (or filtering) in time and space of the velocity field $\boldsymbol{u}$. Leonard (1974) defines the filtered representation of the instantaneous velocity field by convolution integral:

$$\langle u_i(\mathbf{x},t) \rangle_{\ell,\tau} = \int u_i(\mathbf{x}',t') G(\mathbf{x}-\mathbf{x}',t-t') d^3\mathbf{x}' dt' \quad (6)$$

where G denotes the filter kernel which obeys the following relation $\int G(\mathbf{x}-\mathbf{x}',t-t') d^3\mathbf{x}' dt' = 1$. The filter (6) is linear. The filtering operation commutes with time and space derivatives. Germano (1992) showed that contraction of the evolution equation for central moments allows to obtain an equation for the subgrid/modelled kinetic energy. The closed form of the transport equation for the modelled kinetic energy can be written as:

$$\frac{Dk}{Dt} = P_k - F_k \varepsilon + Diff(k) \quad (7)$$

where $P_k=\nu_T S^2$ is the production term, with ν_T the subgrid/modelled viscosity (see definition later) and $S=(2S_{ij}S_{ij})^{1/2}$ invariant of the strain rate tensor. The second term on r.h.s. of eq. (7) is the dissipation $\varepsilon=\beta^* k\omega$ multiplied by the F_k = f(Δ,l_t) function (see definition later). Diff() is the shorthand for diffusion term. The general form of equations presented by Germano (1992) has been considered as a basis for development of the k-ω based hybrid RANS/LES approaches [**H2-H7**]. In particular, the equation (7) was employed for computation of the subgrid turbulent kinetic energy in LES mode of the hybrid techniques. In [**H6**] an additional equation has been derived/adopted for determination of the specific dissipation rate (ω) of the subgrid scales in the PANS method (Partially-Averaged Navier-Stokes), (Girimaji, 2006). The general form of the ω - equation reads:

$$\frac{D\omega}{Dt} = \alpha \frac{\omega}{k} P_k - F_\omega \beta \omega^2 + Diff(\omega) \quad (8)$$

F_ω is again a function allowing to switch between RANS and LES/quasi-DNS modes of the hybrid/PANS model (Table 1). The formula for the subgrid/eddy viscosity can be

written as: $\nu_t=F_v k/\omega$. The F_k, F_v functions are formulated based on the characteristic turbulent length scale l_t (obtained from the modelled transport equations) and the local grid size Δ. The functions were defined in such way that in LES mode the characteristic length scale of subgrid motion was the local grid size Δ, and in RANS mode it was the turbulent length scale, l_t. The applied functions are summarized in Table 1.

The local grid size Δ determines the size of the smallest resolved eddies in a given point of the computational domain using any LES-based technique (including also the studied hybrid models). It means that this characteristic length scale Δ can also be used for estimation of largest unresolved (subgrid) eddies. This estimation is particularly useful for description of the turbulent flow in the inertial range of the cascade, with vanishing role of the turbulence production term. More insight into modelling of the subgrid motion might be gained employing the relation between the subgrid/modelled turbulent kinetic energy k, dissipation rate ε (here interpreted also as the energy transfer), and the size of the local grid size Δ. Such relation can be found using the integral $k = \int_{\kappa_\Delta}^{\infty} E(\kappa)d\kappa$. Assuming the Kolmogorov energy-spectrum function: $E(\kappa) = C_K \varepsilon^{2/3} \kappa^{-5/3}$ (C_K=1.4-1.5, Kolmogorov constant, $\kappa = \pi/l$ is the wavenumber) and setting the cut-off wavenumber to $\kappa_\Delta = \pi/\Delta$ results in:

$$\Delta = \left(\frac{3C_k}{2} \right)^{3/2} \pi^{-1} \frac{k^{3/2}}{\varepsilon} \equiv \frac{k^{3/2}}{\varepsilon} \tag{9}$$

Constant in eq. (9) is 0.97-1.07 (C_K=1.4-1.5), so close to unity. Note that the dissipation ε is kept constant (it is independent of the wavenumber). This approximation is valid for high Reynolds number flows with the cut-off wavenumber placed in the inertial range (Pope, 2000). Eq. (9) allows, therefore, for accurate estimation of the dissipation rate using any LES-like model. However, since LES aims at resolving the scales of motion responsible for turbulence production, it comes into difficulties in near-wall regions, where the size of the eddies is comparable to the Kolmogorov scales, requiring extremely fine grid resolution, approaching that of DNS. In order to alleviate this grid resolution problem in near wall regions, a hybrid RANS/LES can be applied, where the method acts in RANS mode near walls and in LES mode away from walls. It means, that the hybrid model has to switch into the RANS mode in wall vicinity, since formula (9) cannot be employed there (eq. 9 was derived for scales in the inertial range of the cascade). It also means that the fluctuations of dissipation (Frisch, 1995) will be better taken into account in viscosity dominated flow region (near to wall) by the underlying RANS model than by the coarse-grid LES.

In [**H2**] the three versions of the hybrid model were analyzed (Table 1) for simulation of plane impinging jets and for prediction of convective heat transfer along the impingement plate. In the model by Strelets (2001) the destruction term in the k-equation was modified. In the model by Davidson and Peng (2003) and Kok et al. (2004) both the destruction term in the k-equation and the eddy viscosity formula were adjusted. The third model tested was the model by Magnient et al. (2001) and De Langhe et al. (2005a i b). Near to the wall all the hybrid model turned into the RANS mode ($l_t < C_{DES}\Delta$). In this case the standard (RANS) definition of the dissipation term was used in the k-equation (eq. 7), so $\varepsilon=\beta^* k\omega$ (here F_k=1.0,see Table 1). On fine enough grids ($l_t > C_{DES}\Delta$) the hybrid model switched into the LES mode and the dissipation term in eq. (7)

was computed using eq. (9), so $\varepsilon=k^{3/2}/(C_{\mathrm{DES}}\Delta)$, ($\mathrm{F_k}=l_t/C_{DES}\Delta$). An analysis was made for cases with large distance between the slot exit (slot width is denoted by B) and the impingement plate. The normalized distances between the jet exit and the plate were set to H/B=10 for $\mathrm{Re_B}$=13500 and H/B=9.2 for $\mathrm{Re_B}$=20000 (the Reynolds number is based on the slot width). An application of pure RANS model (k-ω model) led to erroneous results both for prediction of the mean flow and the heat transfer characteristics. RANS was in error due to underestimation of turbulence production in the shear layers of the jet. Much better results were obtained using the hybrid models owing to accurate resolution of the vortex breakdown process in LES mode of the hybrid model. Similar results were obtained in [**H3**], where it was demonstrated that the hybrid models, in contrast to RANS models, allow for accurate resolution of the Görtler vortices in the impingement flow region. The numerical results obtained using the hybrid models [**H2, H3**] were in good agreement with the measurements by Mauriel and Soliec (2001), Zhe and Modi (2001), Ashforth-Frosta et al. (1997) and with reference LES results by Beaubert and Viazzo (2003)

The ability of the hybrid models to transfer to the standard Smagorinsky model under equilibrium conditions (production equals to dissipation in the *k*-equation or both in *k*- and ω-equations) was demonstrated, [**H2**, **H3**]. This allowed to obtain a similar subgrid viscosity level in LES mode in both hybrid techniques. Similar analysis was earlier performed by Yan et al. (2005), but aimed at determination of the $\mathrm{C_{DES}}$ model constant. As showed in [**H2**], the transformation of the hybrid RANS/LES model to the Smagorinsky model (equilibrium condition) was not only necessary for an estimation of the underlying LES model constant, but it was also critical for obtaining accurate simulation results. Recently, similar conclusions were drawn by Friess et al. (2015). They showed that it is possible to define a class of *H*-equivalent hybrid RANS/LES models (*H*-equivalence stands for hybrid) for models which have been derived using different hybridization approaches, but giving similar resolved/modelled turbulence levels. Further discussion of this problem was considered in papers [**H4**] and [**H6**] (see description below).

Table 1. Summary of F_{k}, F_{ω} i F_{ν} functions of the hybrid RANS/LES and PANS models ([**H2**, **H3**] and [**H6**]). Turbulent length scale is $l_t=k^{1/2}/(\beta^*\omega)$, $\Delta=\max(\Delta_x\Delta_y\Delta_z)$ is the measure of the local grid size where Δ_x, Δ_y, Δ_z are sizes of the cells in x, y and z directions, C_{DES}=0.67. Constants α, β i β* are given by Wilcox (2008).

Hybrid model	$\mathrm{F_k}$	$\mathrm{F_\omega}$	$\mathrm{F_\nu}$
Model 1 (Strelets)	$\max\left(1,l_t/C_{DES}\Delta\right)$	1	1
Model 2 (Kok)	$\max\left(1,l_t/C_{DES}\Delta\right)$	1	$\min\left(1,C_{DES}\Delta/l_t\right)$
Model 3 (Magnient)	1	1	$\min\left(1,\left(C_{DES}\Delta/l_t\right)^{4/3}\right)$
Model 4 (PANS)	1	$\mathrm{F_\omega}\beta=\mathrm{f_k}\beta+(1-\mathrm{f_k})\beta^*\alpha$	1

In [**H4**] the convective heat transfer was studied for simulation of round impinging jet impacting onto the flat plate. The distance between nozzle exit and plate was equal to H/D=2, 6 and 13.5 (D - nozzle diameter) and the Reynolds numbers were set to:

Re_D=5000, 23000 and 70000 (based on jet diameter and mean velocity at jet exit). The three hybrid RANS/LES models were tested. The first model was the model by Davidson and Peng (2003) and Kok et al (2004), (Table 1), the second was the model by Batten et al. (2004) and the third was a modified model by Davidson and Peng (2003) and Kok et al (2004) (see definition later). Fig. 2 shows a scheme of the computational domain for simulation of impinging jet flow at H/D=2.

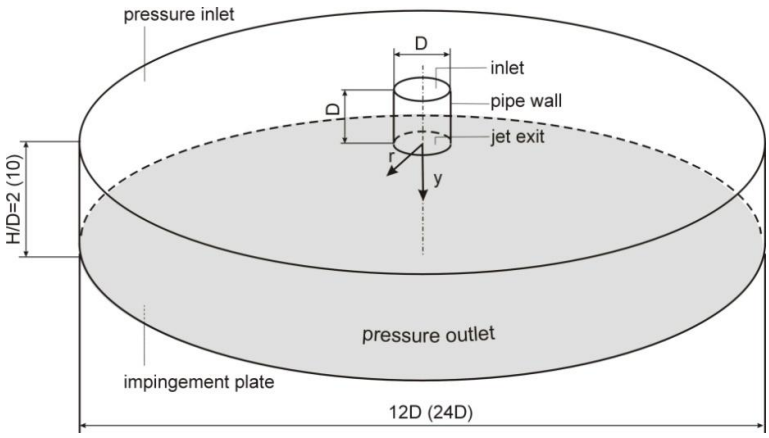

Fig. 2: Scheme of the computational domain for simulation of impinging jet flow at nozzle-plate distance H/D=2.

It was demonstrated [**H4**], that simulation of the round impinging jets at large distance between nozzle exit and plate (H/D > 6) with the RANS k-ω model leads to strong underestimation of the turbulence production in the shear layer of the jet. The deficiencies of RANS model can be cured with application of hybrid RANS/LES models. As mentioned by Durbin (1996), an application of the standard two-equation turbulence models, which in general violate the Schwartz inequality, give a much too high eddy viscosity level in the stagnation flow region. This results in overestimation of the Nusselt number along the impingement plate for cases with small distance between nozzle exit and impingement plate (H/D=2). As showed by Behnia et al. (1998) an application of the standard k-ε model might lead to overestimation of the stagnation point Nusselt number by 100-150%. An application of the k-ω model for simulation of impinging jet flow and heat transfer at small nozzle-plate distance resulted in 20-30% overprediction of the stagnation point Nusselt number [**H4**]. The differences between experiment and prediction were lower than the differences observed using the standard k-ε model (Behnia et al., 1998), but they were still meaningful. In present work [**H4**], an application of the hybrid RANS/LES models was also investigated for simulation of flow and heat transfer in round impinging jets at small nozzle-plate distance (H/D=2) in order to overcome the limitations of the RANS models. Aims of the work [**H4**] were (i) development of boundary conditions for modeled (subgrid) quantities at inlet to computational domain, (ii) analysis of three hybrid RANS/LES models based on the newest version of the k-ω model by Wilcox (2008) in prediction of convective heat transfer in round impinging jet flow, (iii) investigation of the vortex structures dynamics in the impingement zone. An improvement of the model by Davidson and Peng (2003)

and Kok et al. (2004) was also taken into account by employing two definitions of the local grid size: $\Delta=\max(\Delta_x,\Delta_y,\Delta_z)$ and $\Delta_{LES}=(\Delta_x\Delta_y\Delta_z)^{1/3}$. First grid size measure ($\Delta=\max(\Delta_x,\Delta_y,\Delta_z)$) was used in destruction term of *k*-equation, and the second ($\Delta_{LES}=(\Delta_x\Delta_y\Delta_z)^{1/3}$) in the eddy-viscosity formula. Under the assumption of local equilibrium, the eddy viscosity reduced in LES mode to a Smagorinsky subgrid viscosity

$$\nu_t = \left(\left(\beta^*\right)^{3/4} C_{DES} \left(\frac{\Delta}{\Delta_{LES}} \right)^{1/4} \Delta_{LES} \right)^2 S \tag{10}$$

where the Smagorinsky constant $C_s=(\beta^*)^{3/4}C_{DES}$ was set to the standard value 0.1, which gives $C_{DES}=0.6086$. The role of the $(\Delta/\Delta_{LES})^{1/4}$ term was to increase the eddy viscosity level on high aspect ratio cells. With (10), the eddy viscosity expression was similar to the generalised Smagorinsky model proposed by Scotti et al. (1993), to improve the predictive qualities of LES on anisotropic grids. For an isotropic grid, the subgrid viscosity obtained with the modified model is the same as the subgrid viscosity level reproduced with the original model by Davidson and Peng (2003) and Kok et al. (2004).

Jaramillo et al., (2008) showed that a specification of inlet boundary conditions for modelled scalars is critical for simulation of impinging jet flow using RANS models. The present results confirmed this observation also for simulations performed using the hybrid models [**H2**-**H7**]. In all hybrid RANS/LES simulations [**H4**], the vortex method was used to generate resolved perturbations of the velocity field at the pipe entrance located one jet diameter upstream of the nozzle jet exit (Mathey et al., 2006). This allows the flow to adjust before reaching the nozzle exit (Fig. 2). In [**H4**] the inlet conditions (fully developed flow) have been specified according to the measurements by Cooper et al. (1993), Geers at al. (2004), Baughn and Shimizu (1989) and Baughn et al (1991). The full RANS profiles (mean values) of the turbulent quantities were used at the pipe inlet to reproduce the resolved perturbations. With the vortex method, structures smaller than the grid size were not generated at the inlet to the computational domain. So, this means that the modelled part of the total fluctuating velocity was automatically not taken into account. In order to reproduce realistic total fluctuating velocity components at the pipe entrance, the modelled *k* and ω were prescribed. In [**H4**] the boundary conditions for modelled scalars were derived using local equilibrium assumption (Sagaout, 2006). The specification of the accurate boundary conditions for subgrid (modelled) quantities at the inlet boundary was especially important for simulation of low Reynolds number flows using the hybrid models (case with $Re_D=5000$).

The numerical results obtained using the hybrid model were in good agreement with experiment and reference LES. The mean and fluctuating velocities were analyzed in the wall-jet region. For low nozzle–plate distance, the mean velocity profiles were well reproduced by all models. The fluctuating velocity profiles were well reproduced by the hybrid models. RANS overpredicted the fluctuating velocity magnitude in the impact region. For large nozzle–plate distance, again, the hybrid models reproduced the mean velocity profiles very well.

In [**H4**] and [**H5**] the analysis of vortex structures in impingement flow region was performed. Figure 3 shows the contour plots of the Q-criterion ($Q=1/2(\Omega_{ij}\Omega_{ij}-S_{ij}S_{ij})$) defined by Hunt i in, (1998) in the xy-plane with the model by Davidson and Peng (2003) and Kok et al. (2004). The symmetry axis is at x/D=0 and the impingement plate is at (H-y)/D=0. The vertical scale has been magnified in order to show the flow structures in the near-wall region. The dashed curve shows the thickness of the time-

averaged thermal boundary layer, determined as the thickness over which 90% of the temperature difference between the far flow and the plate occurs. Figure 3 (b) shows the near-wall region in range -0.95=x/D=-0.75. Figure 3 (b) illustrates, by means of the perturbation velocity streamlines, a primary vortex and the secondary vortex induced at the wall at x/D=-0.82. The perturbation velocity vector is defined by $\mathbf{v}' = \mathbf{v} - \mathbf{V}$, where $\mathbf{v}$ and $\mathbf{V}$ are instantaneous and mean velocity vectors, respectively. The primary vortices coming from the shear layer of the jet convect in radial direction. Secondary vortices are induced at the wall by the primary vortices. The generation of secondary vortices is mainly visible for r/D>0.5 (|x/D|>0.5), in fig. 3 (a).

The near-wall vortex structures are further examined in Figure 4, with contour plots of the Q-criterion at two distances from the impingement plate (H-y)/D=5% (above the thermal boundary layer) and (H-y)/D=0.5% (inside the thermal boundary layer). The simulations were performed with the hybrid model on coarse (1.4M) and fine (14M) grids. The inner and outer circles denote R/D=1 and R/D=2. Figures 4 (a) and 4 (b) show evidence of broken ring vortices on the coarse grid, but the vortex structures are rather large. This is due to low grid resolution in azimuthal direction. As a consequence, the breakup of the structures into smaller fragments cannot be captured accurately. The flow picture is much more detailed on the fine grid (14M), as demonstrated in Figures 4 (c) and 4 (d). At R/D=0.5-1 the broken ring vortices are visible, breaking up further into smaller streamwise oriented structures. At R/D>2.5 the grid becomes too coarse for resolving the small scale vortex structures. The results demonstrate that the majority of the small scale dynamics, which is relevant for the heat transfer, in the near-wall region in the impact zone of the jet is resolved. This is crucial since application of the pure RANS model gives too high heat transfer rates there, owing to overprediction of the turbulent kinetic energy. It means that the hybrid model better accounts for the stagnation point heat transfer characteristics than the RANS model, providing that sufficiently fine grids are applied there.

Figure 5 shows the Nusselt number along the plate. RANS overpredicts the stagnation point Nusselt number. This is due to overestimation of the eddy-viscosity level in the impact zone. So, the stress limiter does not limit enough. The dashed line with crosses shows the heat transfer rate obtained with a turbulent flow simulation using RANS, but setting to zero the turbulent diffusivity in the energy equation. This result demonstrates that the turbulent diffusion does not play a role in the enhancement of the heat transfer in the stagnation flow region (R/D<1.0), but that it becomes relevant at larger distance from the symmetry axis (R/D>1.0). The stagnation point Nusselt number is better captured by the hybrid models. The minimum in the Nusselt number profile is not captured on the coarse mesh and some improvement is obtained on the fine mesh. The explanation for the secondary peak in the Nusselt number profile is the breakup of the near-wall structures into fine scale turbulence. Clearly, even the finest grid is not fine enough to fully resolve the breakup of the vortices in the shear layer of the jet and in the developing wall jet. So, this test case is computationally very expensive, as a much finer grid would be necessary to reproduce the minimum in the Nusselt number distribution. The experiments by O'Donovan and Murray (2008) and LES results by Olsson and Fuchs (1998) and Hadziabdic and Hanjalic (2008) also showed a significant role of the small-scale structures on the heat transfer process. But the near-wall vortex breakdown, leading to an increased heat transfer around R/D=2 was not fully explained in the cited work. So this aspect was clarified in the current work [**H4, H5**], as explained above.

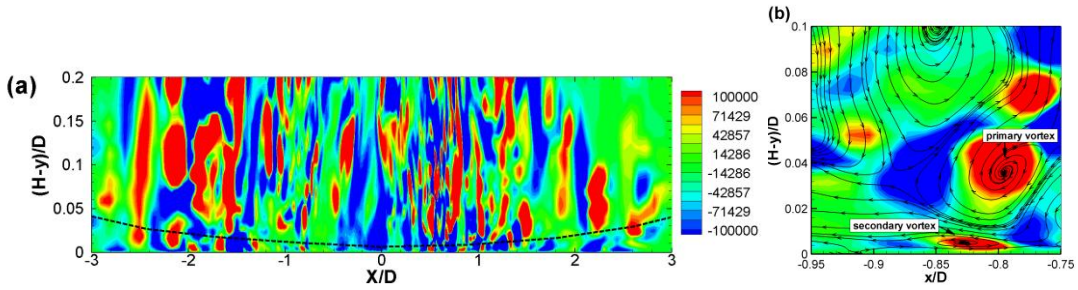

Fig. 3. (a) Instantaneous field of Q-criterion and (b) streamlines of perturbation velocity in the xy-plane at H/D=2, Re=70000 obtained with the hybrid model on the fine mesh (14M), [**H4, H5**]. The dashed line on figure (a) corresponds to the thickness of the time-averaged thermal boundary layer.

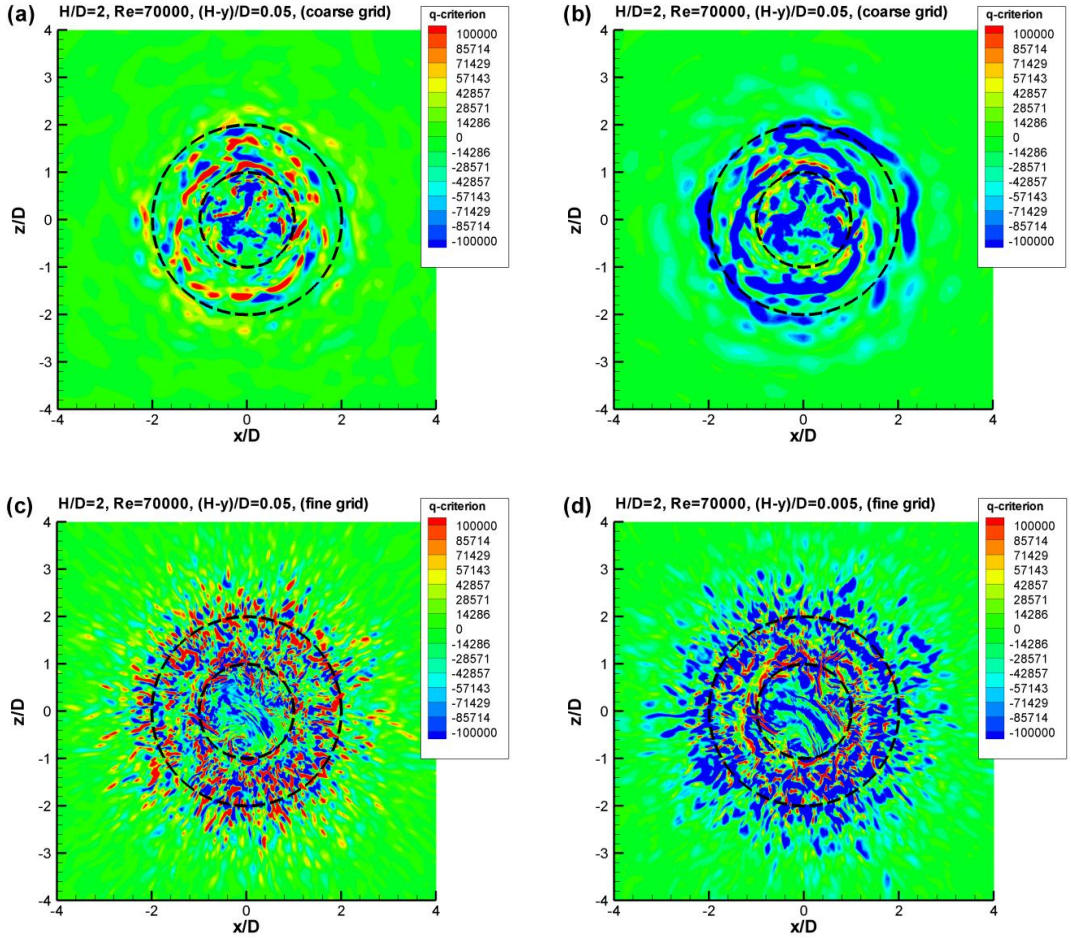

Fig. 4: Instantaneous field of Q-criterion in the xz-plane for H/D=2, Re=70000 obtained with the hybrid model by Kok et al. (2004). Coarse grid: (a) and (b). Fine grid: (c) and (d) [**H4, H5**].

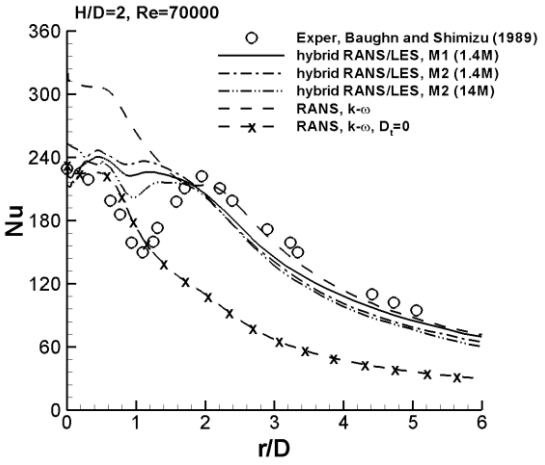

Fig. 5: Nusselt number profile along the impingement plate for H/D=2, Re=70000.

Further analysis of the hybrid RANS/LES models was performed in [**H5**] for simulation of the round impinging jets at different nozzle-plate distances and assuming various Reynolds numbers. The predictive qualities of the hybrid RANS/LES model in LES mode were studied. Tests of the hybrid RANS/LES models by Kok et al. (2004) and Batten (2004) were performed. The basic grid characteristics (1.4 million cells) are illustrated in Fig. 6 for H/D=2, Re=70000 by means of ratio of maximum cell size in radial (a), axial (b) and azimuthal (c) directions and the Kolmogorov length scale, $\eta=(\nu^3/\varepsilon)^{1/4}$. The simulation results have been obtained with the model by Batten et al. (2004). The Kolmogorov length scale is calculated from the dissipation rate, obtained by assuming production equal to dissipation in Eq. (7), following You et al. (2007). Only the modelled dissipation was taken into account, so that we set $\varepsilon = \langle \varepsilon_{SGS} \rangle$. Pope (2000) shows that the scales with sizes $60>\Delta/\eta>8$ are responsible for the bulk of the dissipation. Therefore, it was assumed, following You et al. (2007), that the grid resolution is sufficient in the LES zones of the hybrid model if $\Delta/\eta<40$. As illustrated in Fig. 6 (b), the grid is well refined in y-direction, almost everywhere ($\Delta_y/\eta<40$). This is also true for $|x/D|>3.3$ (results not shown here). Only in small parts close to the pipe $\Delta_y/\eta=40$. For $|x/D|<1$ the grid is sufficiently fine in radial direction ($\Delta_r/\eta<40$), but it is slightly too coarse in the azimuthal direction (inside the pipe and near to the impingement plate $\Delta_\Theta/\eta=60$). Away from the jet axis (for $|x/D|>1$), the grid becomes too coarse for the turbulent eddies to be resolved there. Improved resolution were achieved on the fine mesh (14M), in particular in the azimuthal direction. But in radial direction the grid resolution was still too coarse for $|x/D|>1.5$ even on fine grid (results not showed). It means that the flow dynamics is only barely resolved there when the hybrid model switches into LES mode at some distance from the wall. The turbulent flow dynamics has to be, therefore, modelled in RANS mode of the hybrid RANS/LES model at large distance from the jet axis. So this shows an advantage of application of the hybrid RANS/LES model for simulation of the round impinging jet flow, as the model properly switches from LES to RANS modes in desired flow regions.

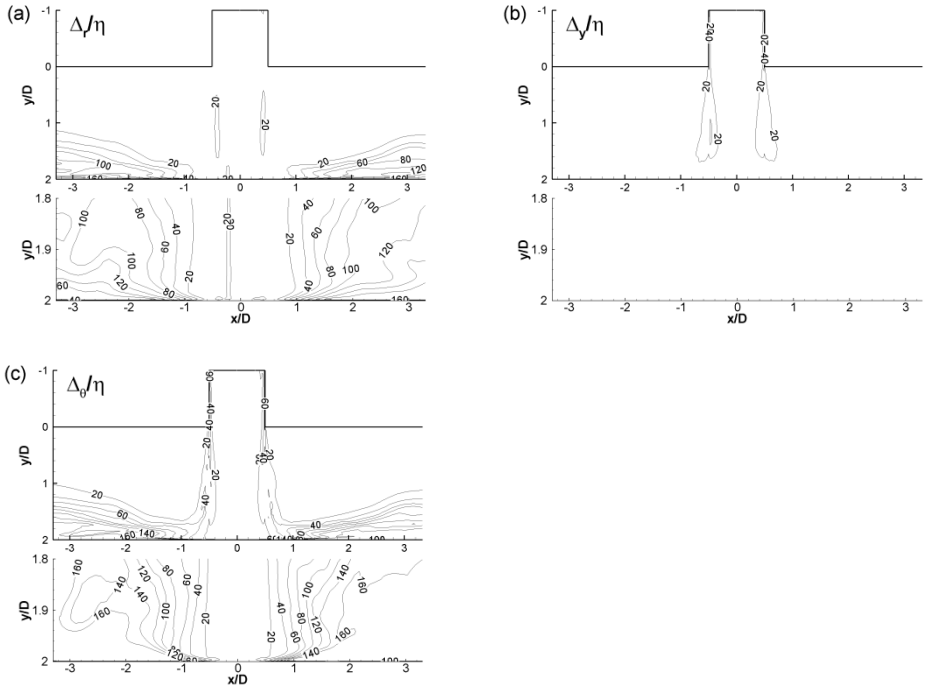

Fig. 6: Grid size normalized with the Kolmogorov length scale (η) in the xy-plane for H/D=2, Re=70000 on basic grid (1.4M), with the hybrid model by Batten (2004), (a) in radial Δ_r/η, (b) wall –normal (axial) Δ_y/η and (c) azimuthal Δ_Θ/η directions.

In [**H6**] an analysis of the hybrid RANS/LES models by Davidson and Peng (2003) and Kok et al. (2004) as well as PANS (ang. Partially-averaged Navier-Stokes) method by Girimaji (2006) was performed for simulation of plane impinging jets. The ω-equation has been derived in [**H6**], using the filtering concept by Girimaji (2006). This allowed, similar to the other hybrid techniques, for application of the k-ω model by Wilcox (2008) in RANS mode of PANS model. In analyzed PANS model, the flow-dependent filter function f_k was applied in order to make a switch between RANS and LES/quasi-DNS modes. With f_k function set to unity the PANS model works in RANS mode, with f_k set to zero the model is not required and quasi-DNS/LES mode is recovered. In the original model by Girimaji (2006) the filter function f_k was simply set to a constant value in the whole computational domain (f_k=0.4). But since application of constant value of f_k filter might change the properties of the underlying RANS model (RANS model was calibrated for f_k=1.0) it was decided to employ the flow-dependent filter function [**H6**] instead of using a constant value everywhere. The filter function was defined as $f_k = \min\left[\left(C_{DES}\Delta_{LES}/l_t\right),1\right]k/k_{tot}$, so it was based on the local grid size $\Delta_{LES}=(\Delta_x\Delta_y\Delta_z)^{1/3}$, the turbulent length scale l_t, the turbulent/subgrid kinetic energy k, and the total turbulent kinetic energy k_{tot} = k + k_{res} (k_{res} denotes the resolved turbulence, k_{res} = ½ $<u'^2+v'^2+w'^2>$, and symbol < > denotes the time averaging). The filter f_k was used for construction of the F_ω function (Table 1), which modified the destruction term in ω-equation (8).

In PANS models it is not possible to impose in a direct way the small-scale Smagorinsky limit on fine enough grids by equating production and dissipation in the k-equation. This is in contrast to the hybrid models by Strelets, Kok and Batten (discussed

above) which impose the Smagorinsky limit under the local equilibrium assumption. The investigation of the predictive qualities of the PANS model on fine enough grids was a subject of work [**H6**].

Fig. 7 (left) shows an evolution of the total Reynolds shear stress at distance y/H=0.5 from the jet exit (half way between the nozzle exit and plate) and fig. 7 (right) shows the skin friction along the impingement plate obtained using various modeling techniques (hybrid RANS/LES model denoted by DES, PANS and pure RANS) for simulation of plane impinging jet at nozzle-plate distance H/B=10 and Re=13500.

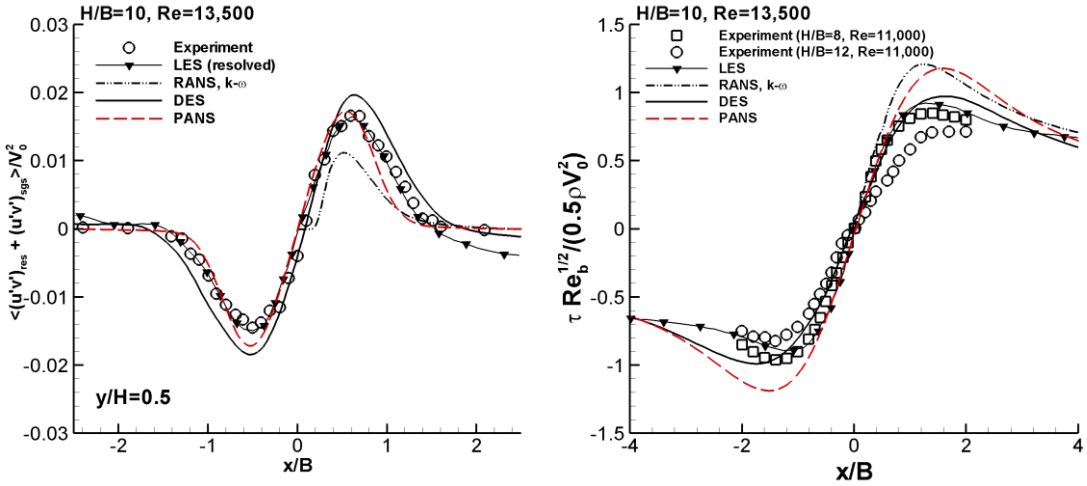

Fig 7: (left) Reynolds shear stress profiles at mid-distance between the jet exit and impingement plate and (right) normalized wall shear stress along the impingement for simulation of plane impinging jet at H/B=10, Re=13500. In reference LES (left) only the resolved shear stress profile is shown.

RANS (2D) seriously underpredicts the turbulence mixing in the shear layers of the jet at y/H=0.5 (Fig. 7, left). The peak value of the shear stress and the width of the shear layer are well captured with both DES and PANS models. One might say that the width is somewhat too small with PANS and somewhat too large with DES. Somewhat too large shear stress level reproduced with DES was probably caused by numerical diffusion (bounded centered scheme was applied for discretization of momentum equations) which delayed the vortex breakdown process. The flow details in the shear layers of the jet have a significant effect on evolution of the wall shear stress along the plate (see fig. 7, right). Note some differences in reference experimental data in fig. 7 (right). PANS produces a too high peak of the wall shear stress, similarly to RANS. This may also be explained by the somewhat too weak turbulent mixing at the outer sides of the jet edges. The break-up of the vortex structures in the outer jet edge regions is too slow. The wall shear stress by the DES model is in good agreement with experiments and LES. The results show that the DES model performs much better than PANS in the developing wall-jet region. Better performance of the DES method was explained by its ability to impose the Smagorinsky limit under the local equilibrium assumption [**H6**]. It means that PANS method stays too close to RANS in a critical flow region and that it is not always possible to overcome the deficiencies of the underlying RANS model

(underpediction of turbulence mixing in developing shear layers) with application of the PANS model.

In [**H7**] an analysis of capabilities of the RANS k-ω model and the modified hybrid RANS/LES model by Kok et al. (2004) in simulation of unsteady three-dimensional flow in a ribbed duct subjected to system rotation was performed. The ribs had a square cross-section and were located on one side of the channel. A correction term for system rotation was introduced into the originating k-ω RANS model. The factor for frame rotation and streamline curvature of Hellsten (1998) was applied in the destruction term of the ω-equation. For consistency reason, the correction term was also introduced in the underlying RANS model of the hybrid technique. The numerical results have been compared with experiments by Coletti and Arts (2011).

Fig. 8 shows the view of the computational domain (flow is from left to right). In Fig. 8, the ribbed duct rotates in counter-clockwise sense around the z-axis with the rotation number $Ro = \Omega D_h/U_0$ set to 0.3 (D_h is the hydraulic diameter and U_0 is the bulk streamwise velocity, both for a cross-section without ribs). The Reynolds number based on U_0 and D_h is Re = 15,000. The clockwise and counter-clockwise rotations of the experiments were simulated by keeping the coordinate frame and the sense of the angular velocity Ω as in Fig. 8, but by turning the computational domain by 180° around the x-axis in order to obtain the clockwise rotation of the experiments.

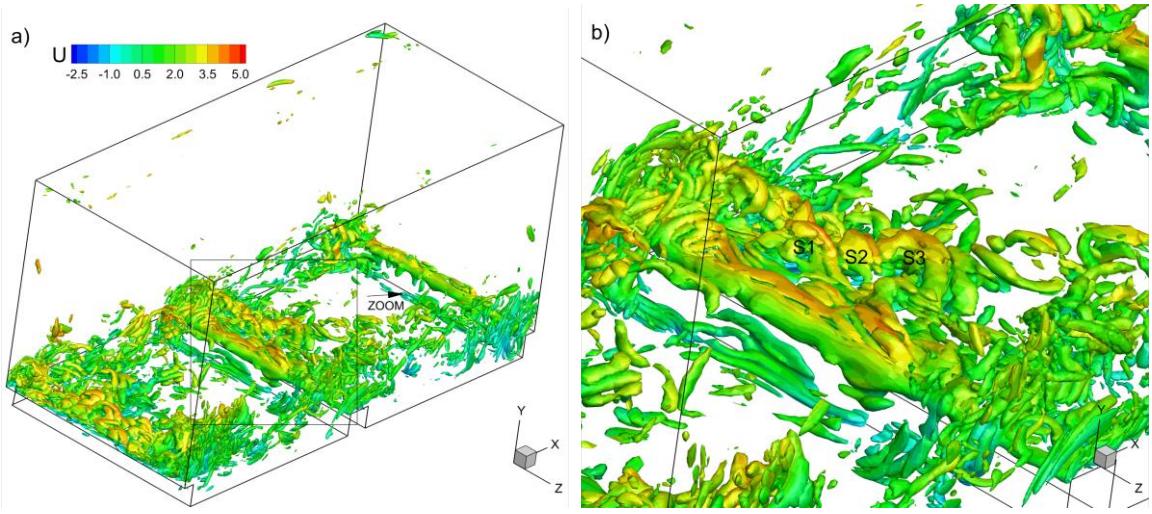

Fig. 8: Counter-clockwise rotation; fine grid (6.1M cells). (a) Vortex structures near the ribbed pressure surface of the duct, visualised by iso-surfaces of q-criterion, $\pm 10^6$, coloured by streamwise velocity; (b) visualisation of hairpin vortices (S1, S2 and S3) in the separated shear layer behind a rib. Flow is from left to right.

The flow was simulated as being periodic in x-direction on a domain of two streamwise modules of the periodic duct, in order to allow detection of flow structures larger than one module. Fig. 8 shows the vortex structures behind the rib (hairpin vortices, denoted as S1, S2 and S3) reproduced with the hybrid RANS/LES model on grid consists of 6.1 million cells. The simulations with coarse grid (2.1 million cells) were also considered in [**H7**]. Fig. 8 shows that the mesh resolution is sufficient (6.1M cells) to capture the flow unsteadiness in LES mode of the hybrid model. Profiles of mean streamwise velocity by the RANS and hybrid RANS/LES models are shown in Fig. 9, along lines perpendicular to the ribbed surface at mid-span at streamwise distances x/H = 0, 2, 4 and 6 behind the

ribs. The results were obtained on the basic grid with 2.1 million cells. The flow statistics were determined by time-averaging.

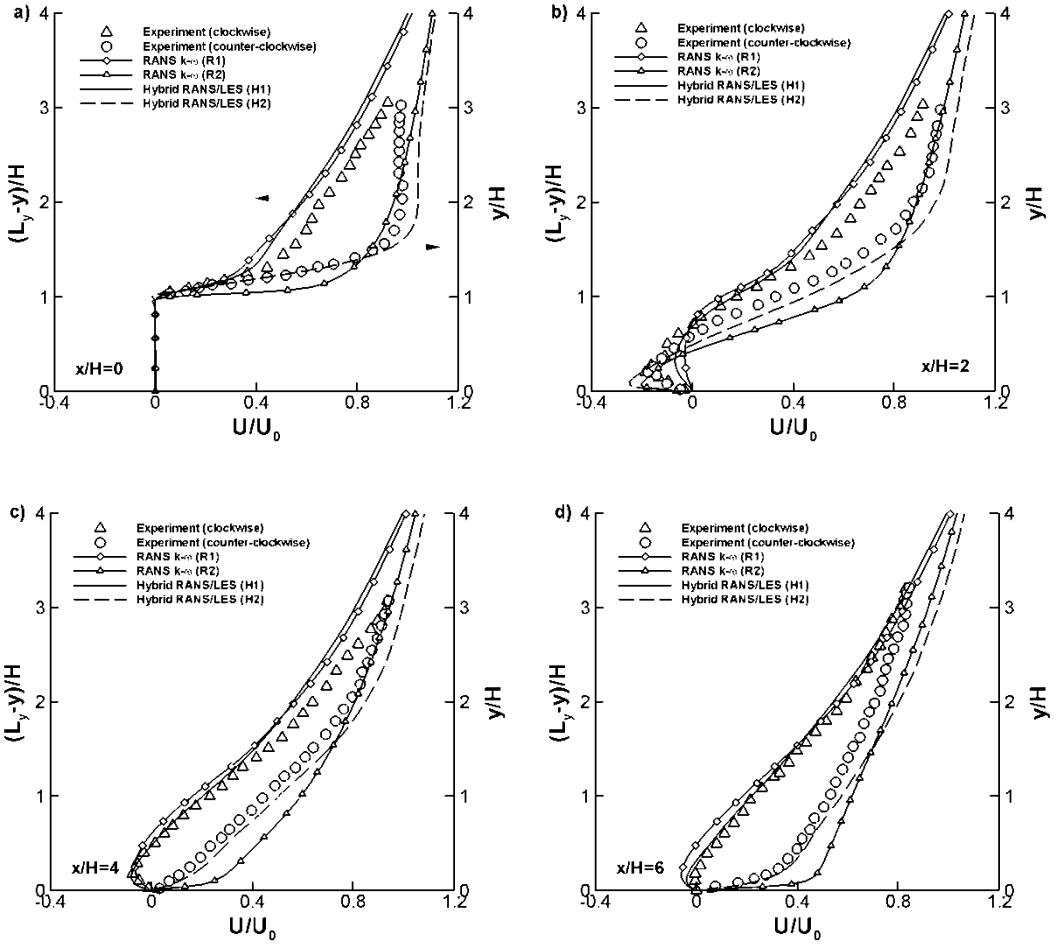

Fig. 9: Profiles of mean streamwise velocity along lines perpendicular to the ribbed surface at mid-span (a) $x/H = 0$, (b) $x/H = 2$, (c) $x/H = 4$ and (d) $x/H = 6$ by the hybrid and RANS models on the basic grid.

Fig. 9 shows that there are no big differences between mean velocity profiles obtained by the RANS and hybrid models and the experimental ones for clockwise rotation (results denoted by R1 and H1, for RANS and hybrid method, respectively). The differences between the results of the RANS and the hybrid models are larger for counter-clockwise rotation. The time-accurate RANS produces a too large velocity gradient at the walls just after the reattachment (Fig. 9 c). This is mainly due to the too large turbulent shear stress predicted by RANS in between the ribs owing to a too much activity of Hellsten correction term there. Results by the hybrid RANS/LES model are, therefore, in much better agreement with experiment than the results obtained using RANS. It has to be stressed that the predictions by the hybrid model are also better in spanwise flow direction (see [**H7**]). In particular, the Coriolis induces secondary vortices are well captured using the hybrid model. With the hybrid model most of the turbulence is resolved, so the role of the Hellsten correction is negligible. The RANS (URANS) model gives erroneous results for simulation of the secondary flow details in spanwise flow

direction in counter-clockwise case. This is due to a too large eddy viscosity level reproduced with URANS on the pressure side of the channel.

The final conclusion is that the hybrid RANS/LES models can be used in analysis of rib-roughened channel flow subjected to system rotation providing sufficient quality grids are employed in the interior of the channel, so majority of the flow dynamics will be resolved there. URANS is quite successful in reproducing the mean flow characteristics in a streamwise flow direction, but is in error in reproducing the secondary flow features in spanwise flow direction.

Modified RANS k-ω model

Durbin and Pettersson-Reif, (2011) and Jaramillo (2008) et al. showed that application of the standard two-equation turbulence models (k-ε, k-ω version from 1998), results in severe overprediction of the stagnation point Nusselt number for prediction of round impinging jet convective heat transfer. The overprediction is due to the fact that the production term in k-equation is proportional to S^2 (S- magnitude of strain rate tensor) while in reality it should be proportional to S in the stagnation flow region (Durbin and Pettersson-Reif, 2011). As result, an application of the standard two-equation models leads to overestimation of the turbulent viscosity level, and also the resulting turbulent diffusivity level, in the stagnation flow region. As mentioned in previous section, this anomaly might also be explained by violation of the Schwarz inequality by the two-equation turbulence models. The two-equation turbulence models which are already supplemented with the stress-limiter like the models by Menter (1994) and Wilcox (2008) allow to bound an overprediction of the eddy viscosity in stagnation flow region and give better heat transfer characteristics. With the SST and new k-ω model the differences between simulation and experiment were about 20-30%. But these differences cannot be accepted in practice (see for instance Aerts et al, 2009). A number of corrections has been proposed in [**H8**] and [**H9**] aiming at improvement of the k-ω model characteristics in the impingement flow region. In [**H9**] two corrections have been suggested. The first correction was based on inclusion of the von Karman length scale in the stagnation flow region. The second was based on inclusion of the Manceau (2003) function. In [**H8**] the modifications were based on application of the Goldberg (2006) and Wilcox (2008) functions. Very good results have been reported in [**H8**] using the modified k-ω model for prediction of heat transfer in round and plane impinging jets at various Reynolds numbers and various nozzle-plate distances. The simulation results were in good agreement with experimental data by Cooper et al (1993), Baughn and Shimizu (1989) and Baughn et l. (1991).

In many engineering applications it is of particular importance to correctly reproduce the mass transfer characteristics at high Schmidt number (Sc=10-1000) using the RANS models. The simulation of high Schmidt number mass transfer process with LES or DNS requires an application of large computational resources, which cannot be afforded in practical use. On the other hand, an application of the standard RANS models which employ the gradient hypothesis for modeling of the diffusion term in the mass transport equations lead to a significant errors. In many electrochemical systems, the Schmidt number is of the order of 1000. As a consequence, in the wall boundary layer, the thickness of the concentration layer is one order of magnitude smaller than the

thickness of the kinematic layer. The mass transfer process is strictly related to the diffusive sublayer and efficiency of this process is controlled by the turbulent motion very close to the wall. So corrections are needed in the near wall region in order to better capture the mass transfer process. A simple algebraic formula was proposed in [**H10**] for simulation of impinging jet mass transfer at high Schmidt numbers. Two variants of algebraic models, based on the limiting behavior of the turbulent diffusivity D_t for $y^+ \to 0$, were employed in order to provide D_t in the near-wall region while away from walls a formula based on the ratio of turbulent to molecular viscosity (ν_t/ν) was applied for determination of the turbulent Schmidt number. Blending between the algebraic expressions and the formula for ν_t/ν is performed in the buffer region of the boundary layer, making the model independent of y^+ at larger distances from the walls. The proposed modifications [**H10**] were based on experimental results by Shaw and Hanratty (1977a, b). The modifications were tested for simulation of the plane impinging jets. Good agreement has been obtained between predictions using proposed model and experiment by Alkire i Ju (1987) and Chin and Agarwal (1991).

Summing up, the proposed stagnation flow correction terms [**H8, H9**] as well as the correction term for the turbulent diffusion in the mass conservation equation [**H10**] were found to be successful and easy to implement. They can be employed in practical simulations of impinging jet heat and mass transfer.

5. Summary of other scientific achievements

In this section, the other research achievements are reported which were not directly related to my PhD thesis entitled: *Parallel computing in analysis of the Navier-Stokes equations using spectral methods*. The outcome of this work has been published in open literature (conference materials, scientific journals or book chapters).

Before obtaining the PhD

Modeling of the laminar to turbulent transition using the intermittency transport model

The research activities were related to development of a novel laminar to turbulent boundary layer transition model based on the intermittency concept. The work was realized during my stay in AEA Technology (now ANSYS), Otterfing, Germany in the period X.2000 do III.2001. The research work was supervised by dr. Florian Menter. My tasks were related to implementation of the computer program for solution of the modified Falkner-Skan equations (boundary layer code). The Falkner-Skan equations were solved together with the supplementary equations for the specific dissipation rate ω and the prototype intermittency function γ. Aim of this study was finding the relationship between the momentum thickness Reynolds number (integral quantity) and the strain-rate based Reynolds number, $Re_S=Sy^2/\nu$ (local quantity). Obtained results were later used for development of the prototype transport equation for intermittency function. The intermittency model was also implemented into the Navier-Stokes code (CFX-TASCFlow) and coupled with the SST k-ω model. The outcome of this work was published in **Menter i in (2002).** The prototype intermittency transport model has been later extended by Langtry and Menter (2006), and the improved model (Langtry and Menter, 2006) is now used in the commercial packages ANSYS Fluent and ANSYS CFX.

Determination of the intermittency factor based on hot-wire data

Research activities focused on analysis of hot-wire signals which have been collected during measurements of the boundary layer flow on suction side of N3-60 blade. The aim was determination of the intermittency factor. The data postprocessing was based on transformation the hot-wire signals (high-pass filtering, differentiation) into the transformed signal (called detector function) which allowed for easier distinction between turbulent and laminar parts. A new technique has been proposed for determination of the threshold value of the detector function. The technique was based on analysis of PDF's of the signals in outer and inner parts of the boundary layer flow. Later on, the obtained threshold value of the detector function was employed for separation of the laminar and turbulent parts of signal and calculation of the intermittency factor. The results of this analysis were presented in conference materials (**Elsner and Kubacki, 2002**). The procedure was later adopted by Jonas et al. (2009). The obtained results were later used by Piotrowski (2007) and Kubacki et al (2009).

After obtaining the PhD

Modeling of the laminar to turbulent flow transition using the dynamic intermittency model

The research activities were devoted to improvement of the predictive qualities of the dynamic intermittency model by Lodefier and Dick (2006) for simulation of wake-induced transition on suction side of N3-60 blade. The dynamic two-equation intermittency model (Lodefier and Dick, 2006) requires an integration of the velocity profiles along the blade surface in order to determine the momentum thickness Reynolds number. In addition, a determination of the edge of the boundary layer for calculation of the local freestream turbulence level and pressure gradient at the edge of the boundary layer is required. The knowledge of above quantities is needed in order to determine both the transition onset and growth rate of turbulent fluctuations in the transition zone. The improvement of the model was based on inclusion of two modifications. The first modification allowed for improved predictions of the transition onset in between wakes. The second modification allowed for faster transition activation in attached boundary layer flow along the leading edge of the wake impacting the blade. Good agreement has been obtained between prediction and experiment by Zarzycki and Elsner (2005) with the modified model. The obtained results have been published in **Kubacki et al. (2009)** and **Dick et al. (2012)**.

Mathematical model for simulation of flow and heat transfer in analysis of electrochemical processes along the plate

The research was devoted to elaboration of mathematical model for simulation of impinging jet flow and convective heat transfer along the plate (aluminum anode) at which the anodic oxide layer was formed. An application of two k-ω models was studied, namely model versions from 1998 and 2006 (see Wilcox). The influence of a variation in convection and applied current density on the local electrode temperatures and oxide thickness was investigated. The analysis showed that the convection plays an important role during the anodizing process. Qualitatively a good agreement was observed between predicted and measured oxide layer thickness. The results has been published in conference materials (**Aerts i in. 2009**) in journal paper **Aerts i in. (2009**) and as a book chapter (**Dick i Kubacki, 2010**).

References

Abu-Ghannam B.J., Shaw R., 1980, Natural transition of boundary layers – the effects of turbulence, pressure gradient, and flow history, J. Mech. Eng. Science, 22: 213-228.

Aerts T., Nelissen G., Deconinck J., Kubacki S., Dick E., De Graeve I., Terryn H., 2009, Aluminium Surface Science and Technology, 5th International symposium,

ProceedingsTemperature and heat transfer during anodizing of aluminium: experiments under applied electrode temperature and numerical simulations, Leiden, Netherlands.

Aerts T., De Graeve I., Nelissen G., Deconinck J., Kubacki S., Dick E., Terryn H., 2009, Experimental study and modelling of anodizing of aluminium in wall-jet electrode set-up in laminar and turbulent regime, Corrosion Science, 51 (7) 1482-1489.

Alkire, R., Ju, J-B.,1987, High speed selective electroplating with impinging two-dimensional slot jet flow, J. Electrochem. Soc., Vol. 134, pp.294–299.

Ashforth-Frost, S., Jambunathan, K., Whitney, C.F., 1997. Velocity and turbulence characteristics of a semiconfined orthogonally impinging slot jet. Exp. Thermal Fluid Sci. 14, 60–67.

Baughn, J.W., Hechanova, A.E., Yan, X., 1991. An experimental study of entrainment effects on the heat transfer from a flat surface to a heated circular impinging jet. Journal of Heat Transfer 113 (4), 1023–1025.

Baughn, J.W., Shimizu, S., 1989. Heat transfer measurements from a surface with uniform heat flux and an impinging jet. Journal of Heat Transfer 111 (4), 1096–1098.

Batten, P., Goldberg, U., Chakravarthy, S., 2004. Interfacing statistical turbulence closures with large-Eddy simulation. AIAA Journal 42 (3), 485–492.

Beaubert, F., Viazzo, S., 2003. Large eddy simulations of plane turbulent impinging jets at moderate Reynolds numbers. Int. J. Heat Fluid Flow 24, 512–519.

Behnia M., Parneix S., Durbin P.A., 1998. Prediction of heat transfer in an axisymmetric jet impinging on a flat plate, Int. J. Heat Mass Transfer 41 (12), 1845-1855.

Brandt L., Schlatter P., Henningson D.S., 2004. Transition in boundary layers subject to free-stream turbulence, J. Fluid Mech. 517:167-198.

Chaouat, B., Schiestel, R., 2005, A new partially integrated transport model for subgrid-scale stresses and dissipation rate for turbulent developing flows. Phys. of Fluids, 17, 065106/1-19.

Chin, D-T. and Agarwal, M., 1991. Mass transfer from an oblique impinging slot jet, J. Electrochem. Soc., Vol. 138, pp.2643–2650.

Coletti, F., Arts, T., 2011, Aerodynamic investigation of a rotating rib-roughened channel by time-resolved particle image velocimetry. Proc. IMechE, Part A: J. Power and Energy. 225, 975-984.

Cooper, D., Jackson, D.C., Launder, B.E., Liao, G.X., 1993. Impinging jet studies for turbulence model assessment-I. Flow-field experiments. International Journal of Heat Mass Transfer 36 (10), 2675–2684.

De Langhe, C., Merci, B., Dick, E., 2005a. Hybrid RANS/LES modelling with an approximate renormalization group. I: model development. J. Turbul. 6 (13), 1–18.

De Langhe, C., Merci, B., Lodefier, K., Dick, E., 2005b. Hybrid RANS/LES modelling with an approximate renormalisation group II: applications. J. Turbul. 6 (14), 1–16.

Dick E., Kubacki S., 2010. Simulation of plane and round impinging jet heat and mass transfer with a RANS $k-\omega$ model for electrochemical applications. & Simulation of plane and round impinging jet heat transfer with $k-\omega$ based hybrid RANS/LES models for electrochemical application. (Eds.) J. Deconinck, A. Hubin, J.P.A.J. van Beeck, VKI Lecture Series, Transport Phenomena in Electrochemical Processes, ISBN-13 978-2-930389-99-0.

Dick E., Kubacki S., Lodefier K., Elsner W., 2012. Intermittency modelling of transitional boundary layer flows on steam and gas turbine blades. Chapter 6 in M.A.R. Sadiq Al-Baghdadi Ed., Engineering Applications of Computational Fluid Dynamics, Vol. 2., International Energy and Environment Foundation, ISBN 978-1478329350, 173-216.

Durbin P.A., 1996. On the k–ε stagnation point anomaly. Int. J. Heat Fluid Flow 17, 89–90.

Durbin P.A., 2012. An intermittency model for bypass transition. Int. J. Heat and Fluid Flow, 36, 1-6.

Durbin i Pettersson-Reif, 2011. Statistical theory and modeling for turbulent flows, John Wiley & Sons.

Elsner W., Kubacki S., 2002, Analiza intermitencji w przepływie przyściennym na powierzchni profilu łopatkowego, XV Krajowa Konferencja Mechaniki Płynów, Augustów, Polska.

Fadai-Ghotbi, A., Friess, C., Manceau, R., Borée, J., 2010. A seamless hybrid RANS-LES model based on transport equations for the subgrid stresses and elliptic blending. Phys. Fluids, 22, 055104/1-19.

Frisch U., 1995. Turbulence. The legacy of A. N. Kolmogorov. Cambridge: Cambridge University Press.

Friess Ch, Manceau R., Gatski T.B., 2015. Toward an equivalence criterion for hybrid RANS/LES methods, Computers and Fluids, 122, 233-246.

Geers L.F.G., Tummers M.J., Hanjalic K., 2004. Experimental investigation of impinging jet arrays. Experiments in Fluids 36, 946–958.

Germano M., 1992. Turbulence: the filtering approach, J. Fluid Mech. Vol. 238, pp. 325-336.

Girimaji S.S., 2006. Partially-Averaged Navier-Stokes model for turbulence: a Reynolds-Averaged Navier-Stokes to Direct Numerical Simulation bridging method, Journal of Applied Mechanics, Vol. 73, pp. 413-421.

Goldberg U., 2006. A k-l turbulence closure sensitized to non-simple shear flows, International, Journal of Computational Fluid Dynamics, Vol. 20 No. 9, pp. 651-6.

Hadziabdic M., Hanjalic, K., 2008. Vortical structures and heat transfer in a round impinging jet. Journal of Fluid Mechanics 596, 221–260.

Hellsten A., 1998, Some improvements in Menter's k-ω SST turbulence model. AIAA-Paper 98-2554.

Hunt, J.C.R., Wray, A.A., Moin, P., 1988. Eddies, Stream, and Convergence Zones in Turbulent Flows, Report CTR-S88, Center For Turbulence Research, Stanford, CA.

Jacobs, R.G., Durbin, P.A., 1998. Shear sheltering and the continuous spectrum of the Orr–Sommerfeld equation. Phys.Fluids 10, 2006–2011.

Jacobs. R.G., Durbin P.A., 2001. Simulations of bypass transition, J. Fluid Mech. 428:185-212.

Jaramillo, J.E., Perez-Segarra, C.D., Rodriguez, I., Oliva, A., 2008. Numerical study of plane and round impinging jets using RANS models. Numerical Heat Transfer, Part B 54, 213–237.

Jonas P., Elsner W., Mazur O., Uruba V., Wysocki M., 2009. Turbulent spots detection during boundary layer by-pass transition, ERCOFTAC Bulletin 80.

Klebanoff, S, 1971. Effect of free-stream turbulence on the laminar boundary layer. Bull. Am. Phys. Soc. 10, 1323.

Kok, J.C., Dol, H., Oskam, H., van der Ven, H., 2004. Extra-large Eddy Simulation of Massively Separated Flows, AIAA Paper 2004-0264.

Kubacki S., Lodefier K., Zarzycki R., Elsner W., Dick E., 2009. Further development of a dynamic intermittency model for wake-induced transition, Flow, Turbulence and Combustion, 83 (4) 539-568.

Langtry R.B., Menter F.R., 2006. A Correlation-based transition model using local variables. Part 1 - model formulation. Proceedings of ASME Turbo Expo 2004 Power for Land, Sea, and Air June 14-17, 2004, Vienna, Austria.

Langtry R.B., Menter F.R., 2009. Correlation-based transition modeling for unstructured parallelized computational fluid dynamics codes, AIAA J., 47: 2894-2906.

Leonard A., 1974. Energy cascade in large-eddy simulations of turbulent fluid flows. Adv. Geophys. 18A, 237-248.

Lodefier K., Dick E., 2006. Modelling of unsteady transition in low-pressure turbine blade flows with two dynamic intermittency equations, Flow, Turbulence and Combustion, 76: 103-132.

Magnient, J.-C., Sagaut, P., Deville, M., 2001. A study of built-in filter for some eddy viscosity models in large eddy simulation. Phys. Fluids 13, 1440–1449.

Manceau R., 2003, Accounting for wall-induced Reynolds stress anisotropy in an explicit algebraic stress model, in: N. Kasagi et al.(Ed.), Proc. Third Int. Symp. on Turbulence and Shear Flow Phenomena, Vol. I., Sendai, Japan.

Maurel, S., Solliec, C., 2001. A turbulent plane jet impinging nearby and far from a flat plate. Exper. Fluids 31, 687–696.

Mathey, F., Cokljat, D., Bertoglio, J.P., Sergent, E., 2006. Assessment of the vortex method for Large Eddy Simulation inlet conditions. Progress in Computational Fluid Dynamics 6, 58–67.

Mayle R. E., 1991. The role of laminar-turbulent transition in gas turbine engines, J. of Turbomachinery 113: 509-537.

Mayle R. E., Schultz A., 1997. The path to predicting bypass transition, J. of Turbomachinery 119: 405-411.

Menter F.R, 1994. Two-equation eddy-viscosity turbulence models for engineering applications, AIAA Journal, 32(8), 1598-1605.

Menter F.R., Esch T., Kubacki S., 2002. Transition modelling based on local variables, (Eds.) W. Rodi, N. Fueyo, Engineering Turbulence Modelling and Experiments, Vol. 5, pp. 555-564, 5th International Symposium on Engineering Turbulence Modelling and Measurements, Mallorca, Spain.

Menter F.R., Smirnov P.E., Liu T., Avancha R., 2015. A one-equation local correlation-based transition model. Flow Turbul. Combust. 95, 583-619.

Moin A.S, Yaglom A., 1971. Statistical Fluid Mechanics, The MIT Press.

Narasimha R., 1957. On the distribution of intermittency in the transition region of a boundary layer, J. Aero. Sci., 24: 711-712.

O'Donovan, T.S., Murray, D.B., 2008. Fluctuating fluid flow and heat transfer of an obliquely impinging air jet. International Journal of Heat Mass Transfer 51, 6169–6179.

Olsson, M., Fuchs, L., 1998. Large Eddy simulations of a forced semiconfined circular impinging jet. Physics of Fluids 10, 476–486.

Pacciani R., Marconcini M., Fadai-Ghotbi A., Lardeau S., Leschziner M.A., 2011. Calculation of high-lift cascades in low pressure turbine conditions using a three-equation model, J. Turbomachinery, 133: 031016/1-9.

Piotrowski W., Elsner W., Drobniak S., 2010. Transition Prediction on Turbine Blade Profile with Intermittency Transport Equation**,** TRANS ASME, J. of Turbomachinery, vol. 132, January, 2010, pp. 011020-1 - 011020-10.

Piotrowski W., 2007. Modeling of laminar-turbulent tranistion using the intermittency function. Praca doktorska. Politechnika Częstochowska. (in Polish)

Sagaut, P., Deck, S., Terracol, M., 2006. Multiscale and multiresolution approaches in turbulence. Imperial College Press, London.

Sandberg R.D., Michelassi V., Pichler R., Chen L., Johnstone R., 2015. Compressible direct numerical simulation of low-pressure turbines—part I: methodology, Journal of Turbomachinery, 137, 051011-1-10.

Savill A.M., 1996. One-point closures applied to transition. Turbulence and transition modelling, M. Hallbäck et al., eds., Kluwer, p. 233-268.

Schiestel R., Dejoan A., 2005, Towards a new partially integrated transport model for coarse grid and unsteady turbulent flow simulations, Theoret. Comput. Fluid Dynamics, 18: 443–468.

Schmidt, R. and Patankar, S., 1991. Simulation Boundary Layer Transition with Low-Reynolds Number k–ε Turbulence Models: Part 2 - An Approach to Improving the Predictions, Journal of Turbomachinery, vol. 113.

Scotti, A., Meneveau, C., Lilly, D.K., 1993. Generalized Smagorinsky model for anisotropic grids. Physics of Fluids A 5 (9), 2306–2308.

Shaw, D.A., Hanratty, T.J., 1977a, Turbulent mass transfer rates to the wall for large Schmidt numbers, AIChE J., Vol. 23, pp.28–37.

Shaw, D.A., Hanratty, T.J., 1977b. Influence of Schmidt number on the fluctuations of turbulent mass transfer to the wall, AIChE J., Vol. 23, pp.160–169.

Spalart P.R, Jou W-H, Strelets M, Allmaras SR, 1997. Comments on the feasibility of LES for wings, and on a hybrid RANS/LES approach. In: Liu C, Liu Z, editors. Advances in DNS/LES. Greyden Press.

Speziale CG., 1996. Computing non-equilibrium turbulent flows with time dependent RANS and VLES. In: 15th international conference on numerical methods in fluid dynamics, Monterey.

Steelant J., Dick E., 1996. Modelling of bypass transition with conditioned Navier-Stokes equations coupled to an intermittency transport equation, Int. J. Num. Methods in Fluids, 23: 193-220.

Strelets, M., 2001. Detached Eddy Simulation of Massively Separated Flows, AIAA Paper 2001-0879.

Suluksna K, · Dechaumphai P, Juntasaro, E., 2009. Correlations for modeling transitional boundary layers under influences of freestream turbulence and pressure gradient, International Journal of Heat and Fluid Flow 30(1):66-75 .

Walters D.K., 2009. Physical interpretation of transition-sensitive RANS models employing the laminar kinetic energy concept. ERCOFTAC Bulletin, 80, 67-71.

Walters D.K., Cokljat D., 2008. A three-equation eddy-viscosity model for Reynolds-averaged Navier-Stokes simulations of transitional flow, J. Fluid Eng., 130: 121401/1-14.

Walters D.K., Leylek J.H., 2004. A new model for boundary layer transition using a single-point RANS approach, J. Turbomachinery, 126: 193-202.

Wilcox, D.C. Turbulence Modeling for CFD. La Canada, CA: DCW Industries, 1992.

Wilcox D.C., 2008. Formulation of the k-ω turbulence model revisited, *AIAA Journal*, Vol. 46, 11, pp. 2823–2837.

Yan, J., Mocket, C., Thiele, F., 2005. Investigation of alternative length scale substitutions in detached-eddy simulation. Flow Turbulence Combust. 74, 85–102.

You, D., Wang, M., Moin, P. And Mittal, R., 2007, Large-eddy simulation analysis of mechanisms for viscous losses in a turbomachinery tip-clearance flow, J. *Fluid Mech.*, Vol. 586, pp. 177–204.

Zaki. T. A., Durbin P.A., 2005. Mode interaction and the bypass route to transition, J. Fluid Mech. 531:85-111.

Zaki T.A., Durbin P.A., 2006. Continuous mode transition and the effects of pressure gradient. J. Fluid Mech 563, 357–388.

Zaki T.A., 2013. From streaks to spots and on to turbulence: exploring the dynamics of boundary layer transition. Flow Turbulence Combust., 91, 451-473.

Zhe, J., Modi, V., 2001. Near wall measurements for a turbulent impinging slot jet. Trans. ASME, J. Fluid Eng. 123, 112–120.

Zarzycki R., Elsner W., 2005. The effect of wake parameters on the transitional boundary layer ona turbine blade. IMechE Part A, J. Power and Energy **219**, 471-480.

Sławomir Kubacki

.....

signature